

EFFECT OF NANO SiC ADDITIVE ON MCMB-SiC COMPOSITE FABRICATION VIA MOLTEN SILICON INFILTRATION

S. Safi¹, R. Yazdani Rad¹, A. Kazemzade¹, Y. Safaei Naeini^{2,*} and F. Khorasanizadeh³

* *yousef.safaei@gmail.com*

Received: January 2012

Accepted: April 2012

¹Ceramic Department, Materials and Energy Research Center, Karaj, Iran.

² Department of Materials, Majlesi Branch, Islamic Azad University, Majlesi, Iran.

³ School of Materials Engineering, Iran University of Science & Technology, Tehran, Iran.

Abstract: C-SiC composites with carbon-based mesocarbon microbeads (MCMB) preforms are new type of high-performance and high-temperature structural materials for aerospace applications. In this study MCMB-SiC composites with high density (2.41 g.cm⁻³) and high bending strength (210 MPa,) was prepared by cold isostatic press of mixed mesophase carbon powder derived from mesophase pitch with different amount (0, 2.5, 5%) nano SiC particles. All samples were carbonized under graphite bed until 1000 °C and finally liquid silicon infiltration (LSI). Microstructure observations resultant samples were performed by scanning electron microscopy and transition electron microscopy (SEM & TEM). Density, porosity and bending strength of final samples were also measured and calculated. Results indicates that the density of samples with nano additive increased significantly in compare to the free nano additives samples.

Keywords: Nano SiC; Composite; Liquid Silicon Infiltration (LSI); Mesocarbon Microbeads (MCMB).

1. INTRODUCCION

Carbonaceous mesophase sphere, as a relevant intermediate product in the liquid carbonization of the pitches or organic compounds, has been recognized as an excellent precursor for high performance carbon materials [1]. The carbonaceous mesophase sphere can be separated from the heat treated isotropic pitch by extraction with a proper solvent according to their solubility difference [2] or high temperature centrifugation [3]. These isolated mesophase spheres have been named as mesocarbon microbeads (MCMB) [3].

Their spherical shape, controlled fusibility and packing flexibility are favorable for making high density and high strength artifacts because MCMB are believed to ensure adhesion among MCMB into the artifact through partial fusion at heat treatment. Their homogeneous shrinkage will not induce the defects in the artifact. Other applications of MCMB, such as a filler of high performance liquid chromatography and lithium ion battery anode, are required to maintain their spherical shape after they are carbonized. The feedstocks, preparation conditions and additives are considered to influence on these properties [4-6].

MCMB separated from heat-treated coal tar and petroleum pitches by quinoline are usually

insoluble and infusible. Their spherical shape can be maintained even though they suffer from a particular shrinkage when they are carbonized and then graphitized, providing the high density of artifacts. On the other hand, the soluble and fusible mesophase has been prepared from hydrogenated coal tar, petroleum pitch or synthetic pitch [7]. MCMB separated from this kind of mesophase may suffer expansion to some extent when they are heat treated. Molecular weight and the content of naphthenic and alkyl groups of mesophase pitch appear to be key factors for controlling fusibility and solubility of MCMB [7].

It has been known in the carbon fiber manufacture process that oxidative stabilization of spun fiber can maintain their fibrous shape in the successive carbonization and graphitization [8]. Oxidative stabilization reactions are believed to be oxidative condensation, oxygenation and oxidative dehydrogenation as well as thermal condensation of the constituent molecules [9]. The fusibility of MCMB can be thus controlled by the stabilization extent. The proper stabilization conditions should be chosen for satisfying packing flexibility, shape stability, adhesion ability and graphitization to make excellent artifacts [9].

Doping foreign materials into MCMBs can also improve the properties and extent of graphitization, or lower the heat treatment temperature of graphitization. Several research results revealed that some refractory-metal carbides (TiC, ZrC, VC and B4C) and elements (B, Si, Ti and Zr) had the catalytic effect, resulting in the improvement of thermomechanical properties [10–11].

C-SiC composites are one of the most important ceramic matrix composites. Modern technology makes wide use of C-SiC composites in different fields, including nuclear reactor walls, pistons for internal combustion engines, battery electrodes, and friction materials [12–17]. These applications exploit the exceptional properties of carbon such as its excellent mechanical behavior at high temperatures, low reactivity, high-heat capacity, and anisotropic thermal conductivity. C-SiC composites are processed according to: (1) a gas phase route, also referred to as chemical vapor infiltration (CVI), (2) a liquid phase route including the polymer impregnation pyrolysis (PIP) and liquid silicon infiltration (LSI) also called (Reactive) Melt Infiltration (RMI or MI) processes as well as (3) a ceramic route, i.e. a technique combining impregnation of the reinforcement with a slurry and a sintering step at a high temperature and high pressure [18]. The reactive melt infiltration (RMI), alternatively called liquid silicon infiltration (LSI) process, is an attractive method for fabricating silicon carbide ceramics due to its lower processing temperature, shorter time and near-net shape fabrication capability [19–28]. The process involves the following steps: fabrication of porous carbon preforms as well as infiltration with liquid silicon and chemical reaction to form silicon carbide ceramics [21,26]. The resulting SiC ceramics are known as Reaction-Formed SiC (RFSC). The morphology and porosity of the preform and the reactivity of the carbon source are the main factors which affect the fabricating process, the microstructures and the mechanical properties of the reaction-formed SiC [20–26].

A novel fabrication approach for C-SiC composites utilizes mesocarbon microbeads (MCMB) as a carbon precursor for preparing porous

carbon preforms. Extracted from mesophase pitch MCMB has been recognized as excellent precursors to parts with high density and strength, and has recently been used as a matrix for carbon-carbon composites [12-13]. The ability of MCMB to self-sinter at relatively low temperatures, homogeneous shrinkage, high yield of carbon, and easy graphitization has attracted considerable attention in the literature [12,13,29–32].

However, no previous studies have been found in the literature using MCMBs as carbon substrate for preparing reaction-formed SiC and relatively few prior studies exists on the effect of nano-SiC powder as dopant on the sintering and properties of MCMBs. In this work, MCMBs with different amounts of nano SiC additive was first used to make a porous carbon preform and then the MCMB-SiC composite was prepared by liquid silicon infiltration. The mechanical and physical properties as well as the microstructure of fabricated MCMB-SiC composite was investigated.

2. Experimental Procedure

2.1. Carbon Porous Preform Preparation

For this study one type of commercially available MCMB (Osaka Gas, Japan), whose characteristics are summarized in Table 1 has been used. First MCMBs were stabilized at 100 °C for 12 h in air. In the following fabrication process, the different amounts of nano-SiC powder was directly doped into the MCMBs, and then mixing and sonicating with magnet stirrer and probe ultrasonic in ethyl alcohol respectively

Table 1. Characteristics of MCMB

Particle Size (μm)	10%<0.66
	50%<5.34
	90%<14.22
Toluene insoluble content (TI) %	95.6
Quinoline insoluble content (QI) %	91.2
β -Resin content %	4.4

were applied in order to get homogeneous mixtures. Then the MCMB- nano SiC mixtures were compacted by cold isostatic press (CIP) under a pressure of 100 MPa. At the same time, the pure MCMBs without dopant were directly molded by cold isostatic press. Carbonization of all the samples were carried out in an electrical furnace with nitrogen atmosphere heated 0.5 °C/min up to 1000 °C.

2. 2. Siliconization Process

Siliconization operation on the porous samples was done at a high-temperature vacuum electric furnace at 1600 °C and 10⁻³ mbar. The specifications

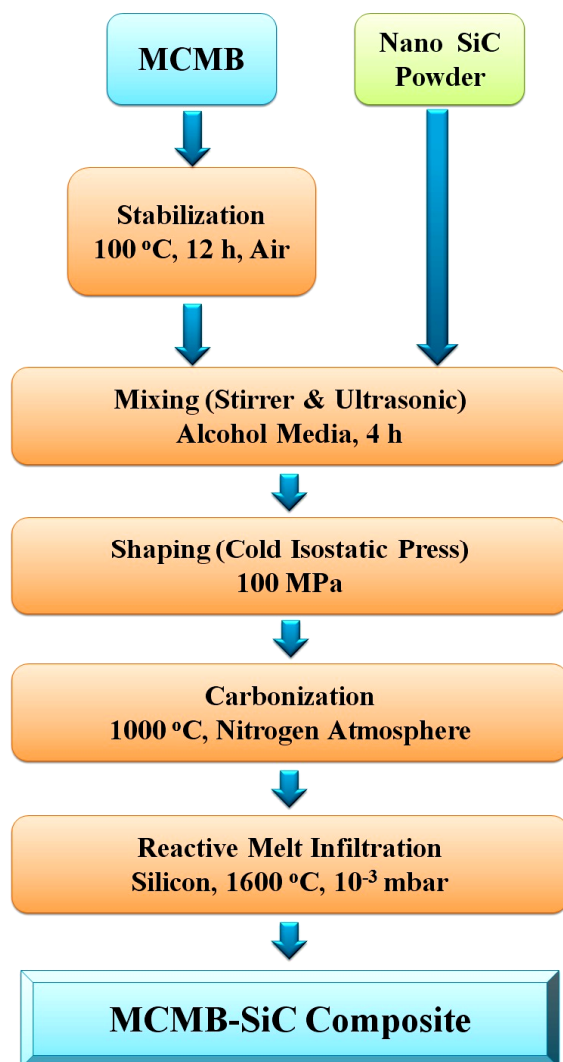


Fig. 1. Processing scheme of manufacturing C-SiC composites

Table 2. Chemical analysis of silicon

%Si	%Ca	%K	%Fe	%Al
98.75	0.3	0.21	0.21	0.53

of silicon used are summarized in Table 2. The fabrication process of the MCMB-SiC composites is also shown in Fig. 1.

2. 3. Characterizations

Morphology of MCMBs and MCMBs- nano SiC powders were considered by transition electron microscope (TEM) before and after mixing. The carbonization process was also analyzed by measuring the mass loss and volume changes of all the specimens. The density and porosity of the carbon porous preform and MCMB-SiC composite was measured by Archimedes' method according to the ASTM C830-91 standard. The flexural strength of the MCMB-SiC composite was measured by three-point-bending test at room temperature on an electron universal testing machine (Gotech Universal). The dimension of the test sample was according to the ASTM C1341-97 standard. Gravimetric analysis was also applied for evaluation of the chemical analysis of the MCMB-SiC composite. To investigate the phase analysis of MCMB-SiC composite, the X-ray diffraction pattern was obtained through Philips pw3710 diffractometer using monochromatized Cu K α radiation ($\lambda=0.1540$ nm). The morphology of polished C-SiC surface was characterized by an optical microscope (OM, Kyowa, Japan) and a scanning electron microscope (SEM, Vega, Tescan, Czech).

3. RESULTS AND DISCUSSION

The TEM micrograph in Fig. 2 (A) show the morphology of the isolated MCMBs with very excellent spherical shape and TEM photograph of the MCMBs with 5 wt.% nano-SiC mixture after ball-milling is shown in Fig. 2 (B).

Particle size distribution of MCMBs with 5 wt.% nano-SiC mixture after ball-milling is also shown in Fig. 3. Morphological change and size reduction of the MCMBs can be seen clearly. The MCMBs

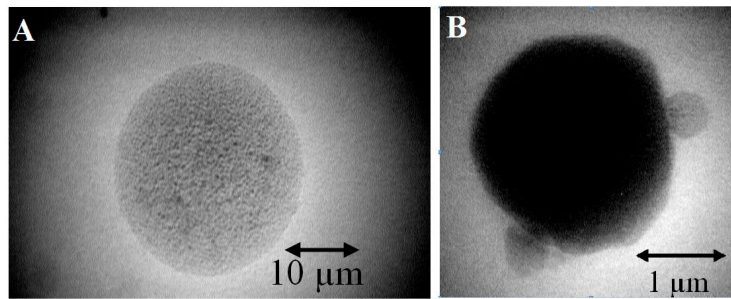


Fig. 2. The TEM micrograph of (A) isolated MCMBs morphology, (B) the MCMBs with 5 wt.% nano-SiC mixture after ball-milling process

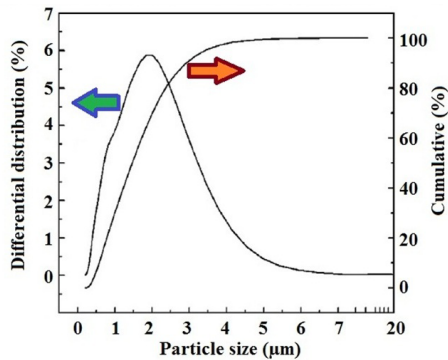


Fig. 3. Particle size distribution of MCMBs with 5 wt.% nano-SiC mixture after ball-milling

spherical particles were broken into smaller grains with a relatively large size distribution ($d_{10} = 2.9 \mu\text{m}$, $d_{50} = 7.3 \mu\text{m}$ and $d_{90} = 14.6 \mu\text{m}$). The SEM micrograph and Si elemental distribution map of a green compact are also presented in Fig. 4. The Si element distributed uniformly, showing a homogeneous distribution of the mixed powders and no nano-SiC agglomerates exist after milling. However, some large pores existed on the surface of the green body, the reason might be that some large broken MCMBs inhibited the homogeneity during

molding.

Fig. 5 shows the linear shrinkage rate of calcined carbon derived from MCMBs (sample 1), MCMBs-2.5 wt.% nano-SiC (sample 2) and MCMBs-5 wt.% nano-SiC (sample 3). It can be seen that the linear shrinkage rate of MCMBs-2.5 wt.% nano-SiC system was lower than MCMBs-5 wt.% nano-SiC system. The highest and lowest linear shrinkage rates, 12.3% and 9.9%, were obtained from the two sintered samples derived from MCMBs-5 wt.% nano-SiC and MCMBs without additive, respectively. Norfolk et al. [33-34] investigated the low-temperature carbonization mechanism and high-temperature graphitization of MCMBs. The sintering involves two main stages: (i) neck formation between particles by a viscous phase non-densifying sintering mechanism ($<527 \text{ }^\circ\text{C}$) and (ii) rapid sample shrinkage due to crystallographic transformations ($527\text{--}927 \text{ }^\circ\text{C}$), so the content of viscous phase was a key factor to volume shrinkage. As we know, the higher content of viscous phase in the green body, the more the amount of volatile matters, and thus the linear shrinkage rate will become higher.

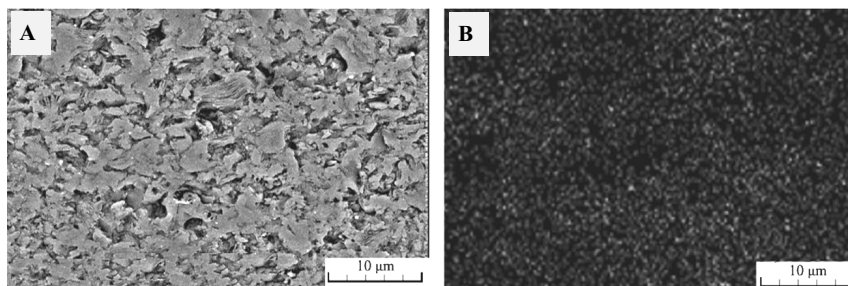


Fig. 4. (A)The SEM micrograph and (B) Si elemental distribution map of a green compact

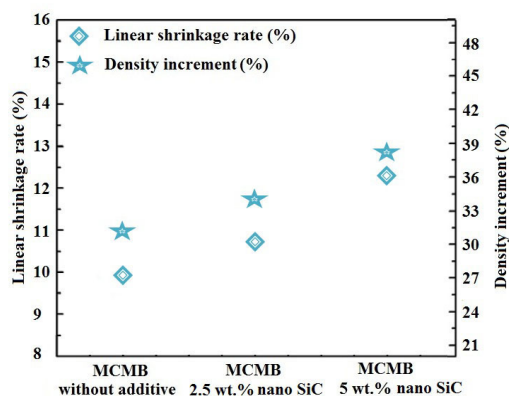


Fig. 5. Linear shrinkage and density change of calcined carbon derived from MCMBs, MCMBs-2.5 wt.% nano-SiC and MCMBs-5 wt.% nano- SiC

Therefore, the calcined carbon derived from MCMBs-5 wt.% nano SiC held the highest linear shrinkage rate because of the maximum content of viscous phase.

Fig. 5 also shows the density increment rate of calcined carbon derived from MCMBs as a function of nano additives amount. The highest density increments of 38.25% was obtained for the system when doped with 5 wt.% nano-SiC. The density of calcined carbon from pure MCMBs was 1.53 g/cm³. When doping with 5 wt.% nano-SiC, the density of MCMBs-SiC samples increased remarkably and the maximum value arrived at 1.87 g/cm³. The change tendency of open porosity was opposite to that of the bulk density. The open porosities of calcined carbon from the MCMBs-5 wt.% nano-SiC system were lower than free additive MCMBs system. The MCMB-5 wt.% nano-SiC sample held the lowest

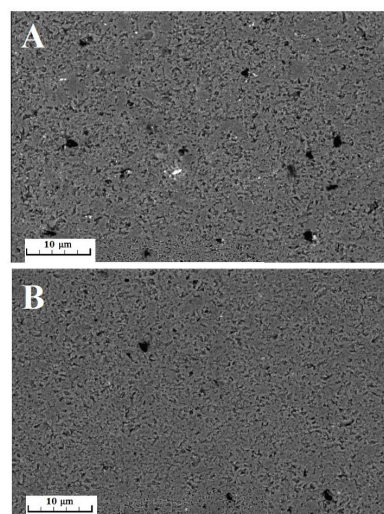


Fig. 6. The SEM photographs of polished surfaces of calcined MCMBs (A) without dopant and (B) with 5 wt.% nano-SiC

open porosity of 8%, corresponding to the highest density value. Fig. 6 shows the SEM photographs of polished surfaces of calcined MCMBs without dopant and with 5 wt.% nano-SiC. There were a lot of pores in the MCMBs sample (Fig. 6A). When doping with 5 wt.% nano-SiC, the calcined carbon became dense and few pores can be seen (Fig. 6B). In addition, although there were some large pores on the surface of the green body (Fig. 4), all the samples became dense after carbonization. Moreover, no cracks were discovered in all the carbonized samples during polishing, indicating that the catalytic effect of nano-SiC can promote particle rearrangement and structure improvement during carbonization.

Table 3. Densities, porosities and bending strengths of carbon performs and C-SiC composites before and after siliconization

samples	Before Siliconization			After Siliconization		
	Density (g/cm ³)	Open porosity %	Bending strength (MPa)	Density (g/cm ³)	Open porosity %	Bending strength (MPa)
1	1.53	15	30	2.32	0.78	210
2	1.67	10.4	67	2.41	0.68	219
3	1.87	8	84	2.53	0.51	232

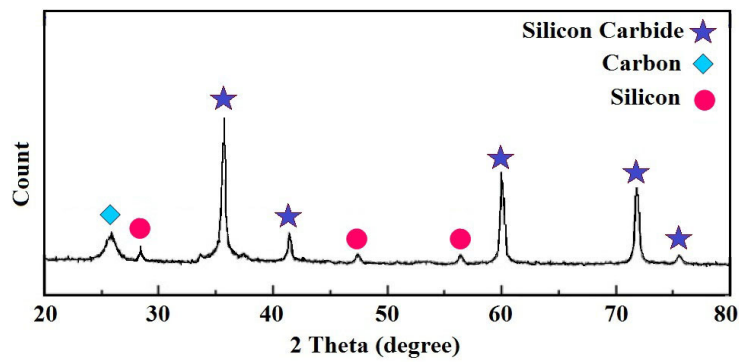


Fig. 7. XRD pattern of C-SiC composite

Table 3 lists the densities, porosities and bending strengths of the preforms before and after siliconization. During the following infiltration processing, molten Si infiltrated into the preforms and reacted with MCMBs-derived carbon to form SiC ceramics. The formed SiC and some residual Si replaced the pores in the preforms, resulting in higher densities and lower porosity of carbon preform after siliconization. A higher bending strength was obtained for siliconized samples.

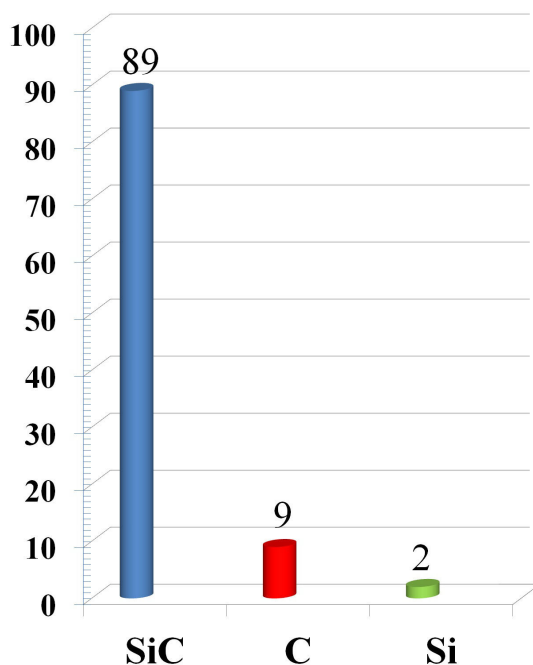


Fig. 8. Chemical analysis of C-SiC composite

The crystal structure of the reaction products was investigated by X-ray diffraction. The XRD pattern of the C-SiC composite is shown in Fig. 7. The phase analysis reveals the presence of carbon, silicon carbide and unreacted silicon in this composite.

Gravimetric analysis was also applied for evaluation of chemical analysis. Unreacted silicon was removed by dissolving the composite in a mixture of 90 volume% nitric acid (HNO_3) and 10 volume % hydrofluoric acid (HF) at 40 °C for 48 h. During the dissolution, elementary silicon first oxidizes to silicon dioxide and subsequently reacts to form a stable hexa fluoro-complex according to the following equations:

The acids only affect free silicon, whereas carbon and silicon carbide remain stable. Due to high accessibility of the SiC zones, the acid reached all the regions of residual free silicon and removed it completely. To remove the carbon completely the samples were exposed to air at 700 °C for 24 h according to the following equations:

The content of each component can be calculated after weighing the residual mass with the result shown in Fig 8.

The microstructural analysis revealed that there was little residual carbon but much SiC produced because of the high activity of the MCMB carbon. A large amount of SiC matrix combined with some residual silicon formed around the dense MCMB grains in the composite (Fig. 9). For porous carbon materials, silicon rapidly infiltrated the carbon preform and reacted with carbon to form SiC during the LSI process. Hence, the macroscopic holes between the

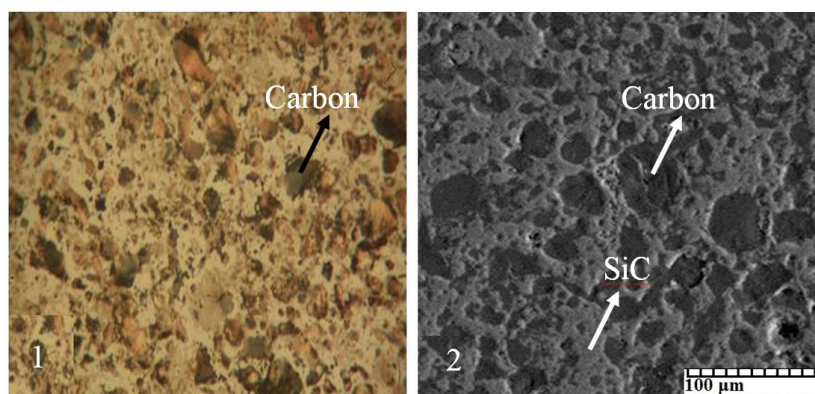


Fig. 9. Micrographs of C-SiC composite 1). Optical microscope 2). SEM microscope.

MCMB grains were filled with SiC, which could also be seen in Fig 9.

4. CONCLUSION

In this study the effect of nano SiC additives on properties of MCMB- SiC composites were investigated. The highest and lowest linear shrinkage rates, 12.3% and 9.9%, were obtained from the two sintered samples derived from MCMBs–5 wt.% nano SiC and MCMBs without additive, respectively. The highest density increments of 38.25% was obtained for the system when doped with 5 wt.% nano-SiC. The density of calcined carbon from pure MCMBs was 1.53 g/cm³. When doping with 5 wt.% nano-SiC, the density of MCMBs–SiC samples increased remarkably and the maximum value arrived at 1.87 g/cm³. The open porosities of calcined carbon in samples with nano additives were reduced. C-SiC composites were fabricated by infiltrating molten Si into the carbon preforms derived from mesocarbon microbeads (MCMB). Siliconized samples have higher densities and lower porosity and higher bending strength. It was established that the composite was composed of 89% β-SiC, 2% C and 9% Si by means of gravimetric analysis.

REFERENCES

1. Bhatia, G., Aggarwal, R. K., Punjabi, N., Bahl, O. P., "Formation of mesophase spherules in low-QI coal tar pitches and development of

- monolithic carbons," *J Mater. Sci.*, 1994, 29, 4757.

2. Yamada, Y., Imamura, T., Kakiyama, H., Honda, H., Fukuda, K., "Characteristics of mesocarbon microbeads separated from pitch," *Carbon*, 1971, 12, 307.
3. Singer, L. S., Riffle, D. M., Cherry, A. R., "High temperature centrifugation: application to mesophase pitch," *Carbon*, 1987, 25, 249.
4. Marsha, H., Foster, J. M., Hermon, G., Iley, M., "Carbonization and liquid-crystal (mesophase) development. Part 2. Co-carbonization of aromatic and organic dye compounds, and influence of inerts," *Fuel*, 1973, 52, 234.
5. Imamura, T., Honda, H., "Formation of carbonaceous mesophase at lower temperature," *Carbon*, 1978, 16, 487.
6. Honda, H., "Carbonaceous mesophase: history and prospects," *Carbon*, 1988, 26, 139.
7. Korai, Y., Mochida, I., "Preparation and properties of carbonaceous mesophase- I Soluble mesophase produced from A240 and coal tar pitch," *Carbon*, 1985, 23, 97.
8. Mochida, I., Toshima, H., Korai, Y., Matsumoto, T., "Enhanced Stabilization Reactivity of Coal Tar Based Mesophase Pitch Fiber by Blending PVC Pitch," *Chemistry Letters*, 1987, 16, 2279.
9. Mochida, I., Korai, Y., Azuma, A., Kakuta, M., Kitajima, E. J., "Layered stacking in the follow carbonization in strictly," *J. Mater. Sci.*, 1987, 26, 4836.
10. Garcia-Rosales, C., Oyarzabal, E., Echeberria, J., Balden, M., Lindig, S., Behrisch, R.,

- “Improvement of the thermo-mechanical properties of fine grain graphite by doping with different carbides,” *Journal of Nuclear Materials*, 2002, 307–311, 1282.
11. López-Galilea, I., Ordás, N., García-Rosales, C., Lindig, S., “Improvement of thermal shock resistance of isotropic graphite by Ti-doping,” *Journal of Nuclear Materials*, 2009, 386–388, 805.
 12. Bhatia, G., Aggarwal, R.K., Punjabi, N., Bahl, O.P., “Effect of sintering temperature on the characteristics of carbons based on mesocarbon microbeads.” *J. Mater. Sci.*, 1997, 32, 135.
 13. Wang, Y. G., Korai, Y., Mochida, I., “Carbon disc of high density and strength prepared from synthetic pitch-derived mesocarbon microbeads.” *Carbon*, 1999, 37, 1049.
 14. Sakagami, S., Iwata, K., Kawase, M., Wakamatsu, S., “Carbon/carbon composite by carbon powder sintering method. In: *Proceedings*,” 1st Japan International SAMPE Symposium, Nov. 28–Dec. 1, 1989.
 15. Schmidt, J., Moergenthaler, K. D., Brehler, K. P., Arndt J., “High strength graphites for carbon piston applications,” *Carbon*, 1998, 36, 1079.
 16. Chen, M. H., Wu, G. T., Zhu, G. M., You, J. K., Lin, Z. G., “Characterization and electrochemical investigation of boron-doped mesocarbon microbead anode materials for lithium ion batteries.” *J. Solid State Electrochem*, 2002, 6, 420.
 17. Blanco, C., Santamaria, R., Bermejo, J., Menendez, R., “Pitch-based carbon composites with granular reinforcements for frictional applications,” *Carbon*, 2000, 38, 1043.
 18. Naslain, R., “Design, preparation and properties of non-oxide CMCs for application in engines and nuclear reactors: an overview,” *Composites Sci and Technology*, 2004, 64, 155.
 19. Chiang, Y. M., Messner, R. P., Terwilliger, C. D., Behrendt, D. R., “Reaction-formed silicon carbide,” *Mater. Sci. Eng. A*, 1991, 144, 63.
 20. Singh, M., Behrendt, D. R., “Microstructure and mechanical properties of reaction-formed silicon carbide (RFSC) ceramics,” *Mater. Sci. Eng. A*, 1994, 187, 183.
 21. Calderon, N. R., Martínez-Escandell, M., Narciso, J., Rodríguez-Reinoso, F., “The combined effect of porosity and reactivity of the carbon preforms on the properties of SiC produced by reactive infiltration with liquid Si,” *Carbon*, 2009, 47, 2200.
 22. Singh, M., Behrendt, D. R., “Reactive melt infiltration of silicon-molybdenum alloys into microporous carbon performs,” *Mater. Sci. Eng. A*, 1995, 194, 193.
 23. Hozer, L., Lee, J. R., Chiang, Y. M., “Reaction-infiltrated, net-shape SiC composites,” *Mater. Sci. Eng. A*, 1995, 195, 131.
 24. Wang, J., Lin, M., Xu, Z., Zhang, Y., Shi, Z., Qian, J., Qiao, G., Jin, Z., “Microstructure and mechanical properties of C/C–SiC composites fabricated by a rapid processing method,” *J. Eur. Ceram. Soc.*, 2009, 29, 3091.
 25. Xu, S., Qiao, G., Li, D., Yang, H., Liu, Y., Lu, T., “Reaction forming of silicon carbide ceramic using phenolic resin derived porous carbon perform,” *J. Eur. Ceram. Soc.*, 2009, 29, 2395.
 26. Wang, Y., Tan, S., Jiang, D., “The effect of porous carbon preform and the infiltration process on the properties of reaction-formed SiC,” *Carbon*, 2004, 42, 1833.
 27. Wilhelm, M., Kornfeld, M., Wruss, W., “Development of SiC–Si composites with fine-grained SiC microstructures,” *J. Eur. Ceram. Soc.*, 1999, 19, 2155.
 28. Wilhelm, M., Werdenich, S., Wruss, W., “Influence of resin content and compaction pressure on the mechanical properties of SiC–Si composites with sub-micron SiC microstructures,” *J. Eur. Ceram. Soc.*, 2001, 21, 981.
 29. Aggarwal, R. K., Bhatia, G., Bahl, O. P., Punjabi, N., “Effect of calcination conditions of self-sintering mesocarbon microbeads on the characteristics of resulting graphite,” *J Mater Sci*, 2000, 35, 5437.
 30. Ozaki, J. I., Nishiyama, Y., “The changes in the structure and some physical properties of mesocarbon microbeads by heat treatment,” *Carbon*, 1987, 25, 697.
 31. Wang, Y. G., Egashira, M., Ishida, S., Korai, Y., Mochida, I., “Microstructure of mesocarbon microbeads prepared from synthetic isotropic naphthalene pitch in the presence of carbon black,” *Carbon*, 1999, 37, 307.
 32. Wang, Y. G., Chang, Y. C., Ishida, S., Korai, Y., Mochida, I., “Stabilization and carbonization properties of mesocarbon microbeads (MCMB)

- prepared from a synthetic naphthalene isotropic pitch,” *Carbon*, 1999, 37, 969.
33. Norfolk, C., Mukasyan, A., Hayes, D., McGinn, P., Varma, A., “Processing of mesocarbon microbeads to high-performance materials: Part I. Studies towards the sintering mechanism,” *Carbon*, 2004, 42, 11–19.
 34. Norfolk, C., Kaufmann, A., Mukasyan, A., Varma, A., “Processing of mesocarbon microbeads to high-performance materials: Part III. High-temperature sintering and graphitization,” *Carbon*, 2006, 44, 301–306.